IOP Publishing Journal of Physics B: Atomic, Molecular and Optical Physics
J. Phys. B: At. Mol. Opt. Phys. **48** (2015) 245001 (5pp) doi:10.1088/0953-4075/48/24/245001

Observing the optical frequency comb in the blue fluorescence of rubidium vapor

Filipe A Lira[1], **Marco P Moreno**[2] **and Sandra S Vianna**[1]

[1] Departamento de Física, Universidade Federal de Pernambuco, 50670-901 Recife, PE–Brazil
[2] Departamento de Física, Universidade Federal de Rondônia, 76900-726 Ji-Paraná, RO–Brazil

E-mail: marcopolo@unir.br

Received 13 June 2015, revised 27 August 2015
Accepted for publication 15 September 2015
Published 23 October 2015

Abstract

We report on the direct observation of the frequency comb printed in the blue fluorescence excitation spectrum of rubidium vapor induced by the combined action of an ultrashort pulse train and a cw diode laser. Each laser drives one step of the 5S—5P—5D two-photon transition in a copropagating configuration and the excitation spectrum is obtained while the cw-laser frequency is scanned over the rubidium D_2 lines. Measurements of the fluorescence as a function of the diode intensity and atomic density allow us to investigate how the effect of power broadening and absorption of the diode laser blur the excitation process. The experimental results and the printing process of the comb on the Doppler profile are described well by numerical integration of the Bloch equations for a cascade three-level system.

Keywords: coherent optical effects, multiphoton processes, atomic spectroscopy

1. Introduction

The frequency comb generated from a mode-locked laser has been established as an important tool for atomic and molecular spectroscopy, where the broadband spectrum consisting of evenly spaced narrow lines is widely exploited [1–4]. In these experiments, a great variety of schemes has been developed, usually based on the use of the frequency comb either as a ruler to measure the frequency of a cw laser, which interacts with an atomic transition, or as a single direct probe of an atomic transition. Specifically, for direct frequency-comb spectroscopy, the two-photon transition is commonly employed. In this case, the resonance condition can be satisfied by many pairs of comb lines, so that the excitation probability can be the same as for a resonant tuned continuous-wave laser of the same average power. However, for atomic systems with broad and crowded spectra, as often encountered with Doppler-broadened profiles, the excitations to different states have to be isolated by the application of narrowband interference filters in the exciting-lasers' pathways [5]. In this context, the introduction of a second, cw, laser opens new directions of investigation, with the narrowband laser assuming the role of a velocity-selective filter. In the case of one-photon transitions, velocity-selective spectroscopy has already been performed [6], and distinction between different hyperfine levels within the Doppler profile has been demonstrated [7].

In this work, we provide a direct observation of the frequency comb printed in the blue fluorescence excitation spectrum of rubidium vapor induced by the combined action of an ultrashort pulse train and a cw diode laser. More specifically, each one of the two copropagating beams at 780 nm (cw) and 776 nm (fs) drives one step of the $5S \rightarrow 5P_{3/2} \rightarrow 5D$ two-photon transition, respectively, and the light emitted from the $6P_{3/2}$ level is detected at 420 nm. In fact, the introduction of a cw diode laser allows us to select the action of the fs laser over only the upper transition. Moreover, with a cw diode laser and a 80 MHz fs laser we observe more than 11 modes within the Doppler profile, instead of using a similar scheme with a 1 GHz fs laser, where a single mode fits within the Doppler profile [8]. We measured the dependence of the blue fluorescence excitation spectra on the Rb density and the input diode laser intensity, which also allowed us to investigate how power broadening and the absorption of the diode laser affect the excitation process.

In our studies, the excitation spectra were obtained as a function of the diode frequency. Although the diode laser can excite all atoms of the Doppler profile, the narrow lines of the frequency comb select only some atomic velocity-groups that can complete the two-photon transition. Therefore, we perform a velocity-selective spectroscopy [6, 7, 9]; where the

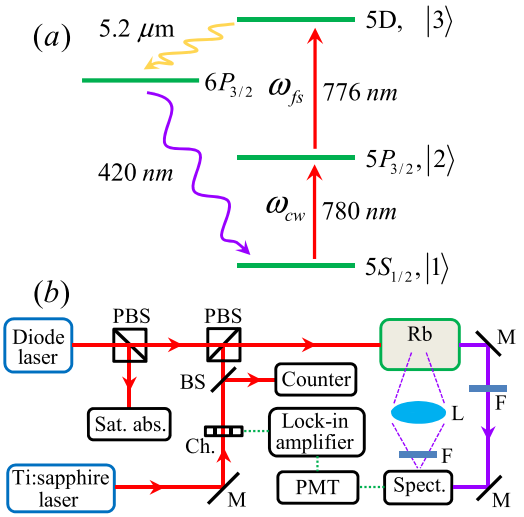

Figure 1. (a) Schematic representation of the relevant energy levels of Rb. (b) Experimental setup. The components are the following: polarizing beam splitter (PBS); photomultiplier tube (PMT); mirror (M); beam splitter (BS); chopper (Ch); filter (F).

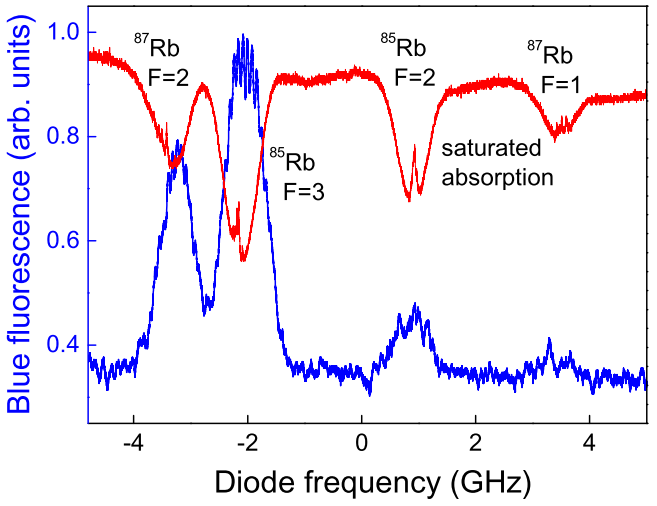

Figure 2. Forward blue emission as a function of the diode frequency for the D_2 Doppler lines. The saturated absorption signal (upper curve) is detected simultaneously.

selectivity, in this case, is defined by the modes in the comb. Direct numerical integration of the Bloch equations for a cascade three-level system is used to analyze the response of the atomic system. The results for the upper level population are calculated for each diode frequency and each atomic group velocity, thereby reproducing the frequency comb printed in the Doppler line profile. Moreover, by taking into account the propagation effects of the diode beam, this approach provides a good description of the additional experimental results.

2. Experimental setup

A simplified scheme of the experimental setup together with the relevant energy levels is presented in figure 1. A diode laser, stabilized in temperature and with a linewidth of about 1 MHz, is used to excite the $5S_{1/2} \rightarrow 5P_{3/2}$ transition. A train of fs pulses generated by a mode-locked Ti:sapphire laser (MIRA, Coherent) can excite both the $5S_{1/2} \rightarrow 5P_{3/2}$ and the $5P_{3/2} \rightarrow 5D$ transitions. The two beams with orthogonal linear polarizations copropagate in a 5 cm long sealed vapor cell, which contains both ^{85}Rb and ^{87}Rb isotopes in their natural abundances and is heated in order to control the atomic density ($T = 40 - 100$ °C).

The Ti:sapphire laser produces 100 fs pulses and 500 mW of average power. The repetition rate of $f_R \approx 76$ MHz is measured with a photodiode and a counter. The fs laser intensity was kept fixed with a mode intensity of the order of 350 μW cm^{-2}. The diode laser can sweep over 10 GHz by tuning its injection current and a saturated absorption setup is used to calibrate its frequency. The diameter of the two beams is almost constant inside the cell and it is about 1.3 mm for the fs beam and 3 mm for the diode laser. The blue light emitted at 420 nm is collected at 90^0 and in the forward direction. Bandpass filters and a spectrometer are used to cut the light around 780 nm. The signal is detected with a photomultiplier tube and recorded on a digital oscilloscope.

3. Results

Figure 2 shows the blue signal intensity detected in the forward direction (lower curve), for a fixed f_R, as the diode frequency is scanned over the four Doppler-broadened D_2 lines of the ^{85}Rb and ^{87}Rb; the saturated absorption curve (upper curve) is used to calibrate the diode frequency. The result was obtained for a cell temperature of 70 °C and a diode beam intensity of $I_d \sim 120$ mW cm^{-2}. The excitation spectrum consists of two intense and two weak broad peaks over a flat background. The broad peaks correspond to the blue light emitted when the two-photon transition is excited by both lasers: the diode laser and the fs laser. The fact that we have two weak peaks, associated with each one of the isotopes, is a consequence of optical pumping. This happens because the smaller F states have greater dipole moments for non-cyclic transitions to the 5P levels. So, for high diode intensity, it makes the fluorescence due to the other ground states be more intense. The background is due to excitation by the fs laser alone. Even though this laser is broad enough to excite both transitions $5S \rightarrow 5P_{3/2}$ and $5P_{3/2} \rightarrow 5D$, we cannot probe its effects by scanning the diode frequency. That is why the signal due to fs laser alone is only a flat background in our results.

A slow scan of the two Doppler lines, $F_g = 3$ of ^{85}Rb and $F_g = 2$ of ^{87}Rb, for different temperatures is shown in figure 3. In these measurements the signal is detected at 90^0 and processed by a lock-in amplifier employing the chopper frequency as a reference. For comparison, the fluorescence signal is normalized to one and we have subtracted the background. Figure 3(a) clearly reveals a structure of peaks whose separation in frequency corresponds to the repetition rate of the fs laser (~76 MHz). Under the conditions of

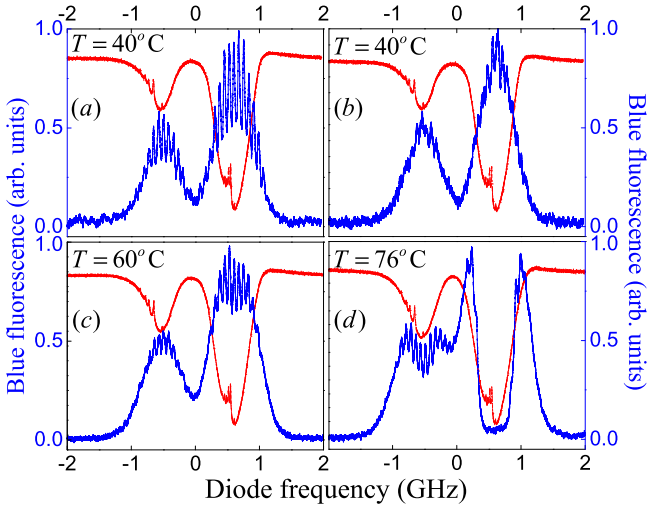

Figure 3. Blue fluorescence detected at 90^0 as a function of the diode frequency, for three different temperatures: (a), (b) $T = 40$ °C, (c) $T = 60$ °C and (d) $T = 76$ °C; and diode intensities: (a) $I_d = 20$ mW cm^{-2} and (b)–(d) $I_d = 60$ mW cm^{-2}.

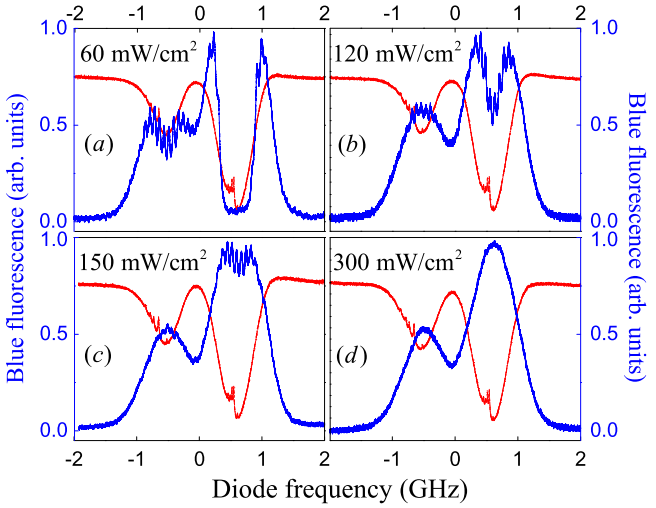

Figure 4. Blue fluorescence detected at 90^0 as a function of the diode frequency, for $T = 76$ °C, and different diode beam intensities.

temperature and diode intensity of figure 3(a), the structure of the peaks is well defined over the two Doppler lines. The peak structure is a demonstration that the atoms are sensible to the frequency comb generated by the mode-locked fs Ti:sapphire laser. It is important to note that this structure of peaks is very similar to that observed in [6], when the frequency comb is printed in the Doppler line profile corresponding to the one-photon transition between 5S to $5P_{3/2}$ states. However, what we see in figure 3(a) is the frequency comb printed in the excitation spectrum of the blue fluorescence from the 6P level. Each peak corresponds to the fluorescence emitted by an atomic velocity group that is simultaneously resonant with the diode laser in the $5S \rightarrow 5P_{3/2}$ transition and with one mode of the frequency comb in the $5P_{3/2} \rightarrow 5D$ transition.

Furthermore, if the diode beam intensity is increased (from $I_d = 20$ mW cm^{-2} to $I_d = 60$ mW cm^{-2} in figures 3(a) and (b)) the resolution of the frequency comb is lost. The blurring of the printed comb can be understood as a result of power broadening on the $5S \rightarrow 5P_{3/2}$ atomic transition by the diode laser. On the other hand, if now we fix the diode intensity and increase the temperature, the comb printed is recovered in the excitation spectrum (figure 3(c)). The reason being that as we increase the temperature, the diode beam is absorbed more throughout the cell and the power broadening effect starts to disappear. However, if the temperature continues to increase, the absorption effect of the diode beam over the $5S(F_g = 3) \rightarrow 5P_{3/2}$ transition of ^{85}Rb is quite strong, and the blue fluorescence goes to zero in the center of this Doppler line, as displayed in figure 3(d). For high temperatures, such as the diode beam is almost entirely absorbed the blue emission is mainly due to the fs laser [10].

The effect of the diode intensity over the blue fluorescence can be better visualized in figure 4, where the temperature was maintained at 76 °C and the diode intensity varied from $I_d = 60$ mW cm^{-2} to $I_d = 300$ mW cm^{-2}. As in figure 3 the fluorescence signal is normalized to one and we have subtracted the background. For low diode intensity, figure 4(a), we repeat the same conditions of figure 3(d) where, together with the strong absorption in the $F_g = 3$ line of ^{85}Rb, we also see a weak absorption in the $F_g = 2$ line of ^{87}Rb. As the diode intensity increases the fluorescence signal, in the center of the lines, also increases (see figures 4(b) and (c)) up to saturation (see figure 4(d)), in which case the power broadening causes the blur of the comb printed in the Doppler lines.

4. Theory

We model our atomic vapor as consisting of independent three-level cascade systems interacting with two fields, which are the cw diode laser field driving the lower transition, $|1\rangle \rightarrow |2\rangle$ ($5S \rightarrow 5P_{3/2}$), and the fs laser driving the upper transition $|2\rangle \rightarrow |3\rangle$ ($5P_{3/2} \rightarrow 5D$). As we are interested in the combined action of the diode and the fs lasers, we neglect the background, by assuming that the fs field does not excite the transition $|1\rangle \rightarrow |2\rangle$.

From Liouville's equation,

$$\frac{\partial \hat{\rho}}{\partial t} = \frac{\mathrm{i}}{\hbar}\left[\hat{\rho}, \hat{H}\right] + (\text{decaying terms}), \tag{1}$$

we obtain the Bloch equations for a group of atoms with velocity v in the rotating wave approximation, by considering the Hamiltonian $\hat{H} = \hat{H}_0 + \hat{H}_{int}$ of the free atom plus the electric dipole interaction:

$$\dot{\rho}_{11} = -\mathrm{i}\Omega_{cw}\sigma_{12} + \text{c.c.} + \gamma_{22}\rho_{22} \tag{2}$$

$$\dot{\rho}_{22} = \mathrm{i}\Omega_{cw}\sigma_{12} + \text{c.c.} - \mathrm{i}\Omega_{fs}\sigma_{23} + \text{c.c.} - \gamma_{22}\rho_{22} + \gamma_{33}\rho_{33} \tag{3}$$

$$\dot{\rho}_{33} = \mathrm{i}\Omega_{fs}\sigma_{23} + \text{c.c.} - \gamma_{33}\rho_{33} \tag{4}$$

$$\dot{\sigma}_{12} = \left(\mathrm{i}\delta_{cw} - \gamma_{12}\right)\sigma_{12} - \mathrm{i}\Omega_{fs}\sigma_{13} + \mathrm{i}\Omega_{cw}(\rho_{22} - \rho_{11}) \tag{5}$$

$$\dot{\sigma}_{23} = \left(\mathrm{i}\delta_{fs} - \gamma_{23}\right)\sigma_{23} - \mathrm{i}\Omega_{cw}\sigma_{13} + \mathrm{i}\Omega_{fs}(\rho_{33} - \rho_{22}) \tag{6}$$

$$\dot{\sigma}_{13} = \left[\mathrm{i}\left(\delta_{cw} + \delta_{fs}\right) - \gamma_{13}\right]\sigma_{13} - \mathrm{i}\Omega_{fs}\sigma_{12} + \mathrm{i}\Omega_{\mathrm{cw}}\sigma_{23} \quad (7)$$

with

$$\rho_{13} = \sigma_{13}\mathrm{e}^{\mathrm{i}\left(\omega_{cw}+\omega_{fs}\right)t} \quad (8)$$

$$\rho_{12} = \sigma_{12}\mathrm{e}^{\mathrm{i}\omega_{cw}t} \quad (9)$$

$$\rho_{23} = \sigma_{23}\mathrm{e}^{\mathrm{i}\omega_{fs}t} \quad (10)$$

$$\delta_{cw} = \omega_{21} - \omega_{cw} - k_{cw}v \quad (11)$$

$$\delta_{fs} = \omega_{32} - \omega_{fs} - k_{fs}v \quad (12)$$

$$\Omega_{cw} = \frac{\mu_{12}E_{cw}(t)}{\hbar}\mathrm{e}^{-\mathrm{i}\omega_{cw}t} \quad (13)$$

$$\Omega_{fs} = \frac{\mu_{23}E_{fs}(t)}{\hbar}\mathrm{e}^{-\mathrm{i}\omega_{fs}t}, \quad (14)$$

where γ_{ij} is the relaxation rate of the matrix element ρ_{ij}, ω_{ij} and Ω_{ij} are the resonance and Rabi frequencies for the transition $|i\rangle \rightarrow |j\rangle$ with electric dipole moment μ_{ij}, and E_{cw} and E_{fs} are the cw and fs fields with wavenumbers and frequencies $k_{cw,fs}$ and $\omega_{cw,fs}$, described by the equations

$$E_{cw}(t) = E_0^{cw}\mathrm{e}^{\mathrm{i}\omega_{cw}t}, \quad (15)$$

$$E_{fs}(t) = \sum_{k=0}^{N-1} E_0^{fs}\left(t - kT_R\right)\mathrm{e}^{\mathrm{i}\omega_{fs}t}. \quad (16)$$

Here, E_0^{cw} is the cw field amplitude, $E_0^{fs}(t)$ is the pulse envelope of the fs field, and T_R and N are the repetition period and the number of pulses.

We assume that the blue fluorescence is proportional to the population of the state $|3\rangle$, ρ_{33}. In all calculations we consider ω_{fs} in resonance with the $|2\rangle \rightarrow |3\rangle$ transition ($\omega_{fs} = \omega_{32}$) and we use $f_R = 1/T_R = 76$ MHz, $T_p = 100$ fs and $E_0^{fs}(0) = 3 \times 10^6$ V m^{-1} ($\bar{\Omega}_{fs} = 0.45\gamma_{33}$), where T_p and $E_0^{fs}(0)$ are the temporal width and the amplitude of the pulses and $\bar{\Omega}_{fs}$ is the Rabi frequency per mode (near the resonance) of the fs field.

The Bloch equations are numerically solved in the time by the classical fourth-order Runge–Kutta method, for each diode frequency and for each atomic group velocity. In order to deal with the Doppler effect, we integrate numerically the density matrix elements over the Maxwell–Boltzmann velocity distribution:

$$\bar{\rho}_{ij} = \int_{-\infty}^{+\infty} \rho_{ij}(v)f(v)\mathrm{d}v, \quad (17)$$

where $f(v)$ is the normalized velocity distribution. We solve this integration numerically by the rectangle method, with velocity intervals of $\Delta v \approx 0.1$ m s^{-1} ($\Delta\delta_{cw,fs} \approx 0.13$ MHz). As this integration is very time consuming, we calculate the density matrix elements for all atomic group velocities in parallel using multiple threads of a graphic processing unit (GPU) [11].

Figures 5(a) and (d) show the numerical results for the upper level population, $\bar{\rho}_{33}$, as a function of the diode frequency, for a very small optical density $\alpha z = 0.01$ (see equation (20)) and diode Rabi frequencies $\Omega_{cw} = 0.5\gamma_{22}$ and $\Omega_{cw} = 1.5\gamma_{22}$, respectively. It is interesting to note that the comb obtained in the Doppler profile is due to a coherent accumulation process, in the upper transition, determined by

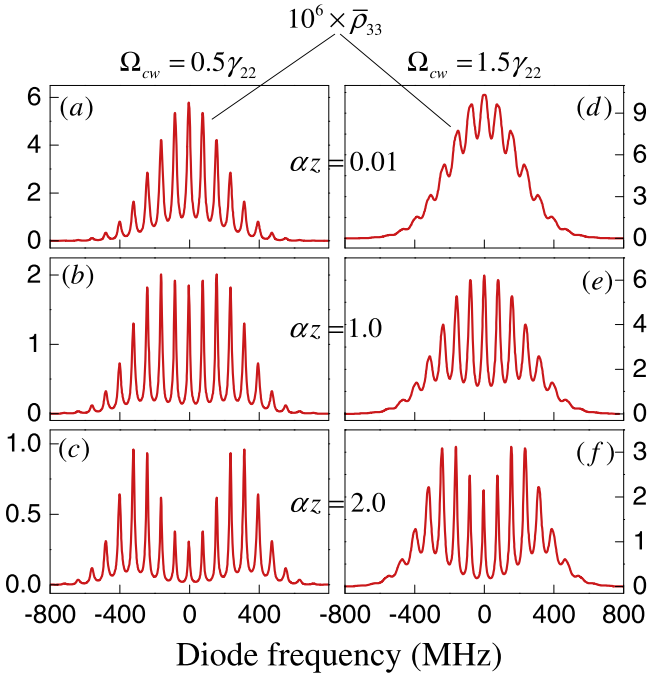

Figure 5. $\bar{\rho}_{33}$ as a function of the diode frequency. Each column shows the result for a specific Rabi frequency and each line for an optical density.

the constructive and destructive interferences between the coherences excited by the sequence of the pulses [12]. Each peak in figure 5 is a result from the following resonance conditions:

$$\omega_{cw} - k_{cw}v = \omega_{21} \quad (18)$$

$$\omega_m - k_{fs}v = \omega_{32}, \quad (19)$$

where $\omega_m = 2\pi m f_R$ is the frequency of the mode m of the comb.

Therefore, each peak represents a two-photon transition driven by the cw field and one mode of the comb, for one atomic velocity group. The decreasing of the visibility of the comb as the diode intensity increase is in concordance with the experimental results displayed in figures 3(a) and (b), and it is explained by the power broadening induced by the diode intensity.

To model the temperature effects we consider the absorption, only of the diode beam, due to the propagation along the Rb cell. We assume that the diode intensity is governed by Beer's law and that the amplitude of the diode field after propagating through the vapor with optical density αz is given by:

$$E_0^{cw}\left(\delta_{cw};\, \alpha z\right) = E_0^{cw}\exp\left[-\alpha z g\left(\delta_{cw}\right)\right], \quad (20)$$

where

$$g\left(\delta_{cw}\right) = \frac{k_{cw}}{\pi}\int_{-\infty}^{\infty}\frac{f(v)dv}{\mathrm{i}\left(\delta_{cw} - k_{cw}v\right) + \gamma_{12}}. \quad (21)$$

For low intensity, figures 5(a)–(c) show us the numerical results for $\bar{\rho}_{33}$ as a function of the diode frequency for three

different values of optical densities: $\alpha z = 0.01$, $\alpha z = 1.0$ and $\alpha z = 2.0$. The reduction of the upper level population and the appearance of a dip at high atomic density is clear (figure 5(c)), similar to that observed in figures 3(c)–(d), due to absorption of the diode field. We present the same results for high intensity in figures 5(d)–(f) and we see the same kind of effect as before. But we also see that we recover the visibility of the comb lines as the optical density increases, as observed in figures 3(b)–(c), because the high absorption of the diode laser along the cell decreases the effect of the power broadening.

It is also interesting to look at figure 5 in a horizontal way, i.e. varying the intensity for a fixed optical density. We already discussed this a little with figures 5(a) and (d), where we saw a decreasing of visibility of the comb lines. The other two pairs 5(b), (e) and 5(c), (f) show that increasing the diode intensity leads to a decreasing of the dip. That was observed experimentally, as shown in figure 4. This is a saturation effect. As the diode laser gets more and more intense, the population $\bar{\rho}_{33}$ will not change much. Therefore, the effect of the absorption will be less pronounced. For a better description, it would be necessary to take into account the saturation effects in the optical density parameter.

Another interesting feature is associated with the linewidth of the peaks inside the Doppler profiles. For low diode intensities, the numerical results give a linewidth for each peak that follows the relation to two copropagating cw beams, on resonance [13], and is limited by the lifetime of both the upper and intermediate levels. The power broadening due to the increasing of the diode intensity is also obtained in our numerical calculations and a good description of the experimental linewidth shown in figure 3(a) is verified.

5. Conclusions

In conclusion, we have investigated the blue fluorescence emitted by an atomic Rb vapor due to the combined action of a cw laser and a train of ultrashort pulses. The frequency comb, that drives the upper transition, is printed in the excitation spectra, and its visibility depends on the laser intensity and atomic density. A good description of the experimental results and the printing process of the comb on the Doppler profile are given by numerical solution of the Bloch equations for a three-level cascade system interacting with both a cw laser and a train of ultrashort pulses.

Acknowledgments

This work was supported by CNPq, FACEPE and CAPES (Brazilian Agencies).

References

[1] Teets R, Eckstein J and Hänsch T W 1997 *Phys. Rev. Lett.* **38** 760
[2] Pe'er A, Shapiro E A, Stowe M C, Shapiro M and Ye J 2007 *Phys. Rev. Lett.* **98** 113004
[3] Barmes I, Witte S and Eikema K S E 2013 *Phys. Rev. Lett.* **111** 023007
[4] Hipke A, Meek S A, Ideguchi T, Hänsch T W and Picqué N 2014 *Phys. Rev.* A **90** 011805(R)
[5] Stalnaker J E, Mbele V, Gerginov V, Fortier T M, Diddams S A, Hollberg L and Tanner C E 2010 *Phys. Rev.* A **81** 043840
[6] Aumiler D, Ban T, Skenderović H and Pichler G 2005 *Phys. Rev. Lett.* **95** 233001
[7] Moreno M P and Vianna S S 2011 *J. Opt. Soc. Am.* B **28** 2066–9
[8] Moreno M P, Nogueira G T, Felinto D and Vianna S S 2012 *Opt. Lett.* **37** 4344–6
[9] Stalnaker J E, Chen S L, Rowan M E, Nguyen Pradhananga T, Palm C A and Kimball D F K 2012 *Phys. Rev.* A **86** 033832
[10] Vujičić N, Ban T, Kregar G, Aumiler D and Pichler G 2013 *Phys. Rev.* A **87** 013438
[11] Demeter G 2013 *Comput. Phys. Commun.* **184** 1203–10
[12] Felinto D, Bosco C A C, Acioli L H and Vianna S S 2003 *Opt. Commun.* **215** 69–73
[13] Bjorkholm J E and Liao P F 1976 *Phys. Rev.* A **14** 751